

# Experimental study of heat transfer to non-Newtonian fluids inside a scraped surface heat exchanger using a generalization method

D. Crespí-Llorens<sup>a</sup>, P. Vicente<sup>a</sup>, A. Viedma<sup>b</sup>

<sup>a</sup>Dep. Ing. Mecánica y Energía. Universidad Miguel Hernández. Av. Universidad, s/n (03202). Elche (Spain). dcrespi@umh.es

<sup>b</sup>Dep. Ing. Térmica y de Fluidos. Universidad Politécnica de Cartagena. Dr. Fleming, s/n (30202). Cartagena (Spain).

---

## Abstract

The heat transfer process to a non-Newtonian pseudoplastic fluid inside a scraped surface heat exchanger has been experimentally analysed. The scraping device consists of a rod with semicircular pieces mounted on it, which are in contact with the inner surface of the pipe. The whole moves axially and thus, the pieces scrape the inner surface of the pipe, in order to avoid fouling formation and enhance heat transfer.

Pressure drop, heat transfer and power consumption measurements, using non-Newtonian pseudoplastic fluids, have been carried out in static and dynamic conditions of the scraper. Four flow regions have been identified: attached laminar, detached laminar, transitional and turbulent flow regions. A generalization method for the fluid viscosity that includes the effects of the non-Newtonian behaviour has been used. Friction factor and Nusselt number have been successfully correlated by employing the generalized viscosity on pressure drop and heat transfer results, both in static and dynamic conditions, for three of the four identified flow regions (it was not possible to get correlations in the transition to turbulent flow region). The study shows that, despite the high power consumption of the scraping movement, the device is suitable for an industrial process using non-Newtonian fluids, since it prevents fouling, increases heat transfer, provides flexibility and enhances the final product quality. Furthermore, the obtained correlations are a valuable tool in the design of heat exchangers.

*Keywords:* heat transfer, non-Newtonian, *Power Law*, experimental, enhanced heat exchanger

---

## 1 Nomenclature

2	$a_i, \dots, e_i$	correlation constants
3	$D, R$	inner diameter and radius of the pipe (Fig. 1)
4	$d, R_s$	diameter and radius of the insert device rod (Fig. 1)
5	$D_h$	hydraulic diameter, $D_h = D - d$
6	$h_i$	film coefficient inside the pipe
7	$h$	constant in function $\Delta$
8	$k$	thermal conductivity
9	$L_p$	pressure ports separation length
10	$m$	flow consistency index (rheological property)
11	$N$	number of experimental measurements
12	$Q$	flow rate
13	$P$	distance from one scraper to the next one at the same angular position
14	$\Delta p$	pressure drop
15	$r$	radial position
16	$t$	scraper length (see Fig. 1)
17	$T$	temperature
18	$U$	uncertainty for a confidence level of 95 %
19	$u$	fluid velocity
20	$u_b$	bulk velocity
21	$v_s$	velocity of the scraper (positive in co-current direction)

## 22 Greek Symbols

23	$\gamma$	shear rate
24	$\mu_g$	generalized viscosity of the flow, $\mu_g = m \phi(n) \left( \frac{u_b}{D_h} \right)^{n-1}$

25  $\rho$  fluid density

26  $\tau$  shear stress

27 **Dimensionless numbers**

28  $\beta$  blockage parameter,  $\beta = 1 - v_s/u_b$

29  $\Delta$  relationship between axial velocity gradients at the heated wall, for a power law fluid and for a Newtonian  
30 fluid

31  $f$  Fanning friction factor,  $f = \Delta p D_h / 2 L_p \rho u_b^2$

32  $n$  flow behaviour index (rheological property)

33  $Nu$  Nusselt number

34  $Pr_g$  generalized Prandtl number,  $Pr_g = c_p \mu_g / k$

35  $Pr_{g,ref}$  reference Prandtl number for one set of experiments.

36  $\phi(n)$  generalization function.

37  $Re_g$  generalized Reynolds number,  $Re_g = \rho u_b D_h / \mu_g$

38  $\omega$  non-dimensional scraping velocity,  $\omega = v_s / u_b = 1 - \beta$

39 **Subscripts**

40  $a$  the device under study (scraper)

41  $av$  section average value

42  $g$  non-dimensional number based on the generalized viscosity

43  $sp$  smooth pipe

44  $dy, st$  dynamic or static scraper respectively

45  $w$  value at the inner pipe wall

## 46 1. Introduction

47 Heat exchangers in the food and chemical industries usually have low efficiency when working with non-Newtonian  
48 fluids. These fluids have high apparent viscosities and therefore, laminar flow at high Prandtl numbers usually occurs.  
49 Moreover, the fouling problem in these heat exchangers has a significant impact on heat transfer inefficiencies and  
50 on cleaning downtime (Beuf et al., 2003; Blel et al., 2013). Besides, high temperature gradients in heated fluids are  
51 common, which decreases the quality of the process and sometimes of the fluid itself.

52 Moving insert devices that scrape the heat exchanger surfaces can be the best option, since they solve some of  
53 the problems that may occur when smooth pipes are employed on high viscous fluids. When the heat transfer surface  
54 is scraped, the heat exchanger is not required to be oversized to take into account the heat transfer decrease due to  
55 fouling. Moving scrapers permit us to work in food or chemical processes without the need of stops that affect plant  
56 productivity. Heating a fluid which is highly mixed, produces a uniform temperature field in the fluid that improves  
57 its quality, which is of the utmost importance in the food industry.

58 Many investigations have focused on scraped surface heat exchangers (SSHE), studying their flow pattern char-  
59 acteristics (Wang et al., 1999), their thermo-hydraulic performance (De Goede and De Jong, 1993) or their scraping  
60 efficiency (Sun et al., 2004).

61 A series of works studied the performance of Newtonian and non-Newtonian flows inside scraped surface heat  
62 exchangers (SSHE) with rotating blades. Mabit et al. (2003) used an electrodiffusion technique in order to investigate  
63 the shear rate on such devices, observing maximum shear rate at the scraping surface and on the leading edge of the  
64 blades. Yataghene et al. (2008) undertook a numerical investigation to characterize the shear rates for Newtonian and  
65 Non-Newtonian fluids. Later, they (Yataghene et al., 2009) studied the effect of index and consistency behaviour of  
66 shear thinning fluid using power-law rheological behaviour on the viscous dissipation through a numerical model.  
67 Finally, they (Yataghene et al., 2011) performed an experimental analysis using Newtonian and non-Newtonian flu-  
68 ids where they studied flow patterns inside a scraped surface heat exchanger (SSHE) with a rotating blade under  
69 isothermal and continuous flow conditions. However, few studies have focused on the analysis of processes using  
70 non-Newtonian fluids within scraped surface heat exchangers (SSHE) with reciprocating scrapers, where the scraping  
71 device moves axially.

72 According to Chhabra and Richardson (2008), pseudoplasticity is the most common non-Newtonian behaviour in  
73 the process industry. Pseudoplastic fluids are characterised by an apparent viscosity which decreases with increasing  
74 shear rate within a certain range of shear rates, and the Power Law model is widely used to represent this behaviour  
75 (Ghannam and Esmail, 1996; Cancela et al., 2005). For such fluids, the friction factor depends on the Reynolds  
76 number and the pseudoplasticity of the fluid, represented in this model by the flow behaviour index  $n$ . Metzner and  
77 Reed (1955) developed a generalization method for smooth pipes which defines a generalized fluid viscosity so that  
78 the friction factor depends only on the Reynolds number defined with such viscosity. Afterwards Kozicki et al. (1966)  
79 and Delplace and Leuliet (1995) extended its use to ducts with uniform cross section.

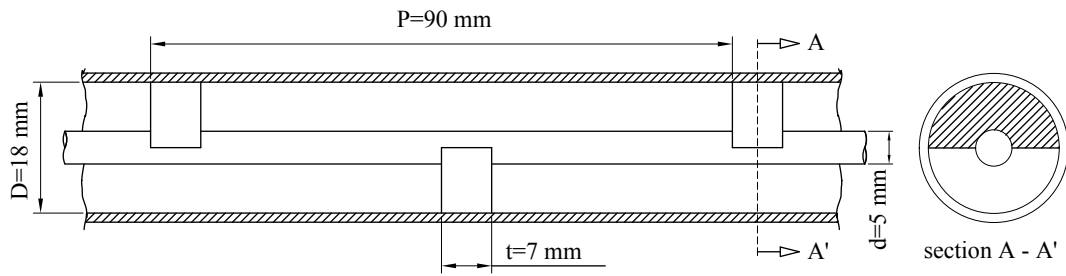


Figure 1: Device under study.

80 Recently, the authors (Crespí-Llorens et al., 2015) defined a generalized viscosity for geometries with non-uniform  
 81 cross section in static conditions of the scraper and also studied the flow pattern in static and dynamic conditions  
 82 (Crespí-Llorens et al., 2016). In this research, the generalization method of the former work has been applied to the  
 83 moving scraper. Experimental results will show the possibilities of applying this non-dimensional methodology, that  
 84 simplifies and generalizes the study of the mechanical and thermal problems.

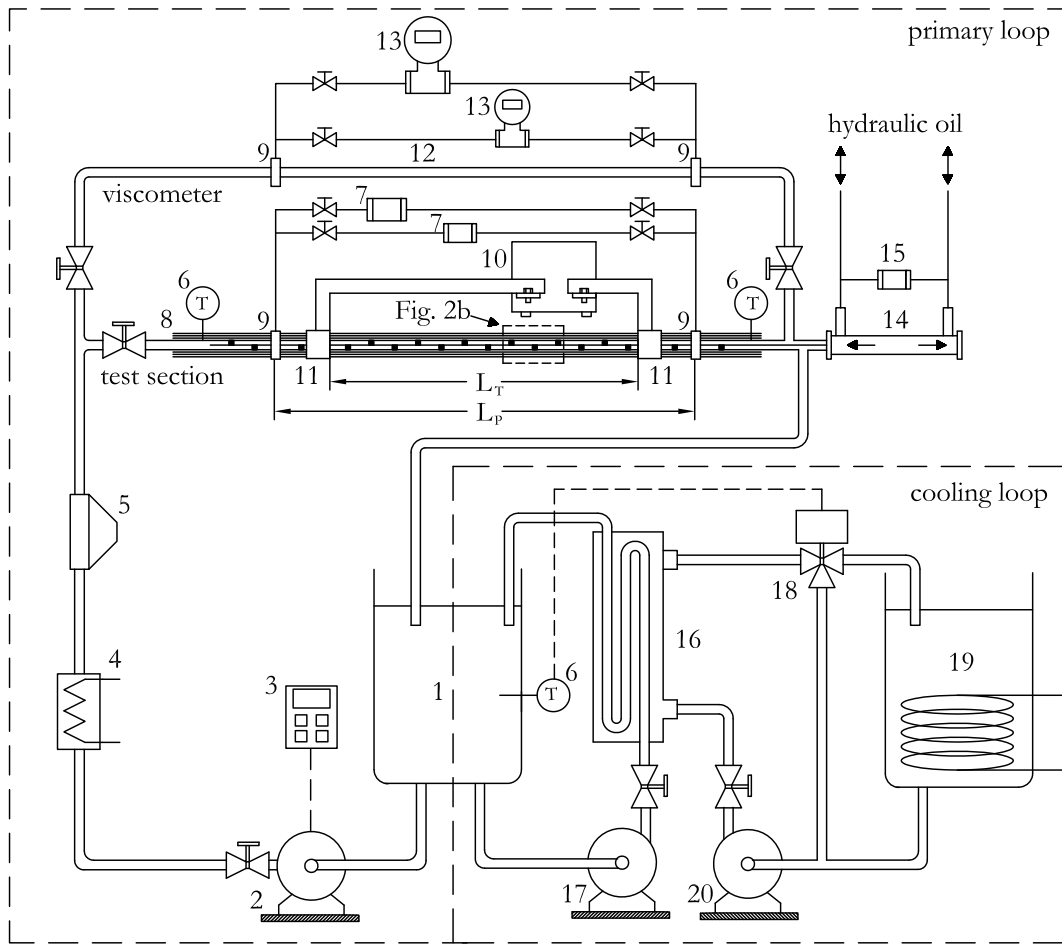
85 This work presents an experimental study of the heat transfer process to a pseudoplastic non-Newtonian fluid in  
 86 a tubular SSHE. The scraper is shown in Fig. 1 and consists of semicircular shaped devices mounted on a moving  
 87 rod. A hydraulic cylinder impels the whole alternatively along the axial direction and the device scrape the internal  
 88 wall of the tube. The movement can be done sporadically to remove fouling, in that case, the study of the device  
 89 in static conditions (static scraper) will be enough to evaluate its performance. In other cases, it will be better to  
 90 actuate the scraper continuously at different velocities in order to increase heat transfer. In these situations, the power  
 91 consumption of the movement has to be considered in the energy balance.

92 The research has two objectives. The first is to evaluate the performance of the device under study, which works  
 93 with non-Newtonian fluids. For that, pressure drop, heat transfer and power consumption have been measured as  
 94 functions of the involved variables: Reynolds number, Prandtl number and scraping velocity. The second objective is  
 95 to evaluate the applicability of a generalization method for the viscosity of a power law fluid to the case of a moving  
 96 scraping device.

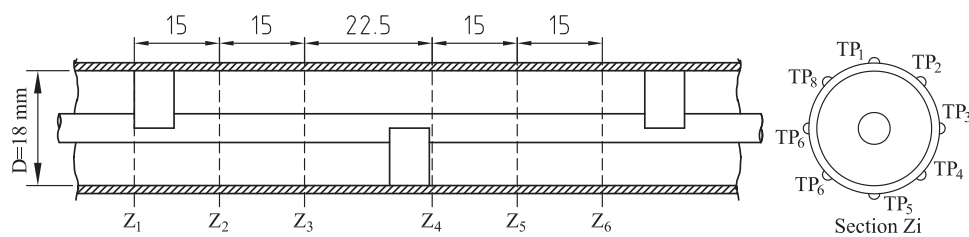
97 Friction factor and Nusselt number have been correlated by employing the generalized viscosity on pressure  
 98 drop and heat transfer results, both in static and dynamic conditions. Finally a performance evaluation of the heat  
 99 transfer enhancement has been calculated to determine the negative effect of the power consumption for the scraping  
 100 movement.

## 101 2. Experimental Setup

102 The experimental set-up shown in Fig. 2(a) has been used to measure pressure drop, heat transfer and the moving  
 103 rod power consumption for different flow regimes and scraping velocities.



(a) Experimental set-up.



(b) Thermocouple distribution along the test section.

Figure 2: Experimental set-up. (1) Test fluid tank, (2) primary loop gear pump, (3) frequency converter, (4) immersion resistance, (5) Coriolis flowmeter, (6) RTD temperature sensor, (7) non-stationary differential piezoresistive pressure transmitters, (8) stainless steel tube with an insert scraper and with inlet and outlet immersion RTDs, (9) pressure taps, (10) electric transformer, (11) electrodes, (12) smooth stainless steel pipe used as viscometer, (13) stationary pressure transmitters, (14) hydraulic piston, (15) non-stationary bidirectional differential piezoresistive pressure transmitter, (16) heat exchanger, (17) cooling loop gear pump, (18) three-way valve with a PID controller, (19) coolant liquid tank, (20) centrifugal pump.

104 *2.1. Experimental set-up description*

105 The experimental facility consists of two circuits:

- 106 • *The primary loop*, containing the test section (8) and the viscometer (12) in parallel
- 107 • *The cooling loop*, which controls the temperature of the test fluid in the main tank(1).

108 The primary circuit can be manually configured to circulate the flow either through the test section or the viscome-  
109 ter.

110 The test section consists of a 4 m long, 2 mm thick, 18 mm internal diameter, 316L stainless steel tube with an  
111 insert device with the geometry shown in Fig. 1. A low-velocity gear pump (2) is used to circulate the working fluid.  
112 Such a type of pump has been selected to minimize fluid degradation during the experiments. A Coriolis flowmeter  
113 (5), which has been reported to perform properly when working with non-Newtonian fluids (Fyrrippi et al., 2004),  
114 measures mass flow rate and fluid density. The pressure drop is measured at pressure taps separated  $L_p = 1.8$  m  
115 ( $20 P$ ). An entry region  $L_e = 0.54$  m ( $6 P$ ) long, ensures fully developed periodic flow conditions. Each pressure  
116 connection (9) is composed of four boreholes separated  $90^\circ$ . Two non-stationary differential piezoresistive pressure  
117 transmitters Kistler 4264A (7) of ranges 0 – 2 bar and 0 – 5 bar have been used with this aim. The devices perform  
118 with an accuracy of 0.05% F.S.

119 The pressure drop of the fully developed stable flow within the viscometer is measured by means of two highly  
120 accurate stationary pressure transmitters SMAR LD301 (13) which are configured for different ranges.

121 With the aim of carrying out thermal experiments under uniform heat flux (UHF) conditions, two copper electrodes  
122 have been installed in the thermal test section, so that the heat is produced at the tube wall through the Joule effect.  
123 Power is supplied by a 6 kVA transformer (10), connected to a variable auto-transformer for power regulation. The  
124 distance between both electrodes is  $L_T = 1.0$  m ( $11 P$ ). The total power transferred to the test section is obtained  
125 by measuring the voltage (0-15 V) and the electrical current (0-600 A). The pipe loop has been heavily insulated to  
126 minimize heat losses. The pipe outside wall temperature is measured by means of 48 K-type thermocouples distributed  
127 in six axial positions as shown in Fig. 2(b), where the first section is located a distance of 0.54 m ( $6 P$ ) downstream  
128 the first electrode. Fluid inlet and outlet temperatures are measured by two Resistance Temperature Detectors (RTDs)  
129 class B 1/10 DIN.

130 A hydraulic cylinder (14) propels the scraper in its axial movement. The pressure in the cylinder chambers is  
131 measured by a non-stationary bidirectional differential piezoresistive pressure transmitter of 0-20 bar (15), which  
132 allows us to determine the hydraulic system power consumption.

133 The test fluid temperature is controlled at the test fluid tank (1). Cooling is provided by the cooling loop (items 16  
134 to 19) in Fig. 2(a)), which uses an oversize gear pump (17) to circulate the test fluid through a cooling heat exchanger  
135 (16). On the other side of the exchanger, the flow rate of the coolant fluid is controlled by a three-way-valve and a  
136 PID controller (18), which controls the temperature of the test fluid tank.

137 *2.2. Test fluid characteristics*

138 A 1% wt aqueous solution of SigmaAldrich Co. carboxymethyl cellulose (CMC) has been used as test fluid. CMC  
139 powders with different chain length have been used.

140 The solutions have been prepared by dissolving the polymer powder in distilled water and then raising the pH  
141 values of the solution to increase viscosity. This fluid shows a non-Newtonian pseudoplastic behaviour which can be  
142 described by the *Power Law* model for a wide range of shear rates (Abdelrahim and Ramaswamy, 1995; Ghannam  
143 and Esmail, 1996; Abu-Jdayil, 2003; Yang and Zhu, 2007).

$$\tau = m\gamma^n \quad (1)$$

144 As per the studies of Chhabra and Richardson (2008); Cancela et al. (2005), all CMC thermophysical properties  
145 except for the rheological parameters and fluid density have been assumed to be the same as pure water.

146 The type of CMC powder employed, the preparation method and fluid degradation due to shear stress and thermal  
147 treatment influence strongly the rheological fluid properties. This allows us to obtain fluids with different pseudo-  
148 plastic behaviour,  $m \in [4.6; 0.016]$  Pa s<sup>n</sup> and  $n \in [0.43; 1]$ . The rheological properties of the non-Newtonian test  
149 fluid  $n$  and  $m$  are measured by the viscometer (item 10 in Fig. 2(a)). This procedure has been explained in detail  
150 previously (Crespí-Llorens et al., 2015). The maximum uncertainty of the measurements of  $n$  and  $m$  are 0.01% and  
151 0.4% respectively.

152 **3. Experimental methodology**

153 In order to simplify the analysis of the flow, a generalization method for the fluid viscosity has been used, which  
154 provides an expression for the parameter  $\phi(n)$  in Eq. 2. The resulting generalized viscosity is used for the definition  
155 of the Reynolds and Prandtl numbers,  $Re_g$  and  $Pr_g$ .

$$\mu_g = m \phi(n) \left( \frac{u_b}{D_h} \right)^{n-1} \quad (2)$$

156 The definition of  $\phi(n)$  for the geometry under study (Fig. 1) was provided by Crespí-Llorens et al. (2015) for static  
157 conditions of the scraper,

$$\phi(n) = 262.27^{n-1} n^{-2.1177} \quad (3)$$

158 Besides, in Section 6, the definition of  $\phi(n)$  by Metzner (1965) is used for the smooth pipe geometry.

159 A correction factor for non-Newtonian fluids has been applied to obtain correlations free from variable property  
160 effects (Joshi, 1978; Joshi and Bergles, 1980).

$$Nu = \frac{h_i D_h}{k} \left( \frac{m_{av}}{m_w} \right)^{0.44n-0.58} \quad (4)$$



161 Besides, in order to simplify the study, a parameter  $\Delta^{1/9}$  is used to account for the influence of the non-Newtonian  
 162 behaviour in the Nusselt number (Grigull, 1956; Martínez et al., 2014).

$$\Delta = \frac{\left(\frac{\partial u}{\partial r}\right)_{r=R, n \neq 1}}{\left(\frac{\partial u}{\partial r}\right)_{r=R, n=1}} = \frac{24n + h}{(24 + h)n} \quad (5)$$

163 In this work, the value of  $h = 7.532$  is used for the annulus geometry, which has been obtained by means of the  
 164 numerical model described previously by the authors (Crespí-Llorens et al., 2016).

165 For both pressure drop and heat transfer measurements, the experiments in both static and dynamic conditions  
 166 have been carried out in sets and the rheological properties have been measured at the beginning and the end of each  
 167 set.

168 In Section 6.1, the performance of the device is compared to the performance of pure forced convection inside  
 169 a smooth pipe. The behaviour of non-Newtonian fluids in the reference geometry has been obtained by a numerical  
 170 model.

171 The uncertainties have been calculated according the "Guide to the expression of uncertainty in measurement",  
 172 published by the ISO (1995). The uncertainty of  $Re_g$  and  $Pr_g$  depend strongly on the uncertainty of the experimental  
 173 generalization method, being 11% for both parameters. The uncertainty of the Fanning friction factor  $f$  and the  
 174 Nusselt number  $Nu$  are 1% and 2%, respectively.

#### 175 4. Pressure drop results in dynamic conditions

176 For experiments in dynamic conditions, the scraper moves continuously in co-current and counter-current direc-  
 177 tions. A full cycle is defined as the time taken by the scraper to make its co-current movement and its counter-current  
 178 one. Both half cycles have been studied separately in section 4.1 and the average pressure drop of the full cycle is  
 179 studied in section 4.2.

##### 180 4.1. Pressure drop in co-current half cycle and in counter-current half cycle

181 In this section, pressure drop has been measured in the co-current and the counter-current movements of the  
 182 scraper separately. Previous visualization studies (Crespí-Llorens et al., 2016), have found the structure of the flow to  
 183 be strongly dependent on the blockage of the flow, defined as follows:

$$\beta = 1 - v_s/u_b \quad (6)$$

184 In particular three different structures were identified for the following values:  $\beta > 0$ ,  $\beta = 0$  and  $\beta < 0$ . The flow  
 185 velocity pattern for  $\beta = 0$  is intermediate between the other two, being almost equal to the flow in annulus geometry.  
 186 Being the case of the static scraper ( $\beta = 1$ ) a case of positive blockage, the flow structure is similar to other cases  
 187 with  $\beta > 0$ . From Eq. 6, these cases occur for  $v_s < u_b$ , and thus, for low scraping velocities in both directions or  
 188 counter-current direction in any case.

Table 1: Pressure drop experimental correlation constants in dynamic conditions. Laminar flow.

	(a) Pressure drop on each scraping half-cycle (Eq. 7).		(b) Full-cycle average pressure drop (Eq. 9).		
	co-current	counter-current	$a_2$	$b_2$	$U(f)$
$a_1$	44.93	40.63	39.52	-0.9558	14.6 %
$b_1$	-0.9593	-0.9307			
$c_1$	0.4624	0.54			
$U(f)$	15.4 %	14.2 %			

189 A total of 450 experiments have been carried out for  $Re_g \in [1; 200]$  and  $\beta \in [0.2; 2.5]$ . The rheological prop-  
 190 erties of the different fluids which have been used in the experiments are within the ranges  $n \in [0.43; 1]$  and  
 191  $m \in [4.26; 0.016]$  Pa s<sup>n</sup>.

192 As stated before, the two different half cycles of the scraping movement (each with a different value of  $\beta$ ) have  
 193 been studied separately. On the one hand, pressure drop results in the co-current direction of the scraping movement  
 194 are shown in Fig. 3 for experiments with  $\beta = 0.5, 0.7, 0.8, 0.9$ . For the experiments with  $\beta = 0.9$ , the flow is laminar  
 195 up to  $Re_g \approx 110$ , where the transition occurs. For the experiments with a lower value of  $\beta$ , the transition region is not  
 196 observed that clearly, due to the lack of results for high Reynolds numbers. On the other hand, pressure drop results  
 197 in the counter current direction are shown in Fig. 4 for experiments with  $\beta = 1.1, 1.2, 1.3, 1.5, 2, 2.5$ . As it can be  
 198 appreciated, for higher values of  $\beta$ , the transition is reached at lower Reynolds numbers. However, for the experiments  
 199 with higher  $\beta$ , the transition is not reached due to experimental limitations.

200 The results in the laminar region have been correlated with Eq. 7 for co-current and counter-current scraping  
 201 directions. The values for the constants of the equations for both cases are detailed in Table 1(a) and the correlation is  
 202 shown in Fig. 3 and Fig. 4.

$$f = a_1 Re_g^{b_1} \beta^{c_1} \quad (7)$$

203 In both scraping directions, the results show the expected increase in pressure drop as the *blockage of the flow*,  $\beta$ ,  
 204 increases.

205 Besides, the assumption of the validity of the generalization method for the cases with  $\beta > 0$  has been confirmed,  
 206 as the friction factor  $f$  in experiments with different fluid characteristics has been found to follow the same correlation  
 207 with  $Re_g$ .

#### 208 4.2. Full cycle average pressure drop

209 In standard operation conditions, the scraper works in full cycles with a constant value of  $|v_s|$ , being  $v_s$  negative  
 210 for the counter-current half-cycle and positive for the co-current one. Consequently, the study of the average pressure  
 211 drop for the full cycle of the scraper movement has been found of interest. In this case, the non-dimensional scraping

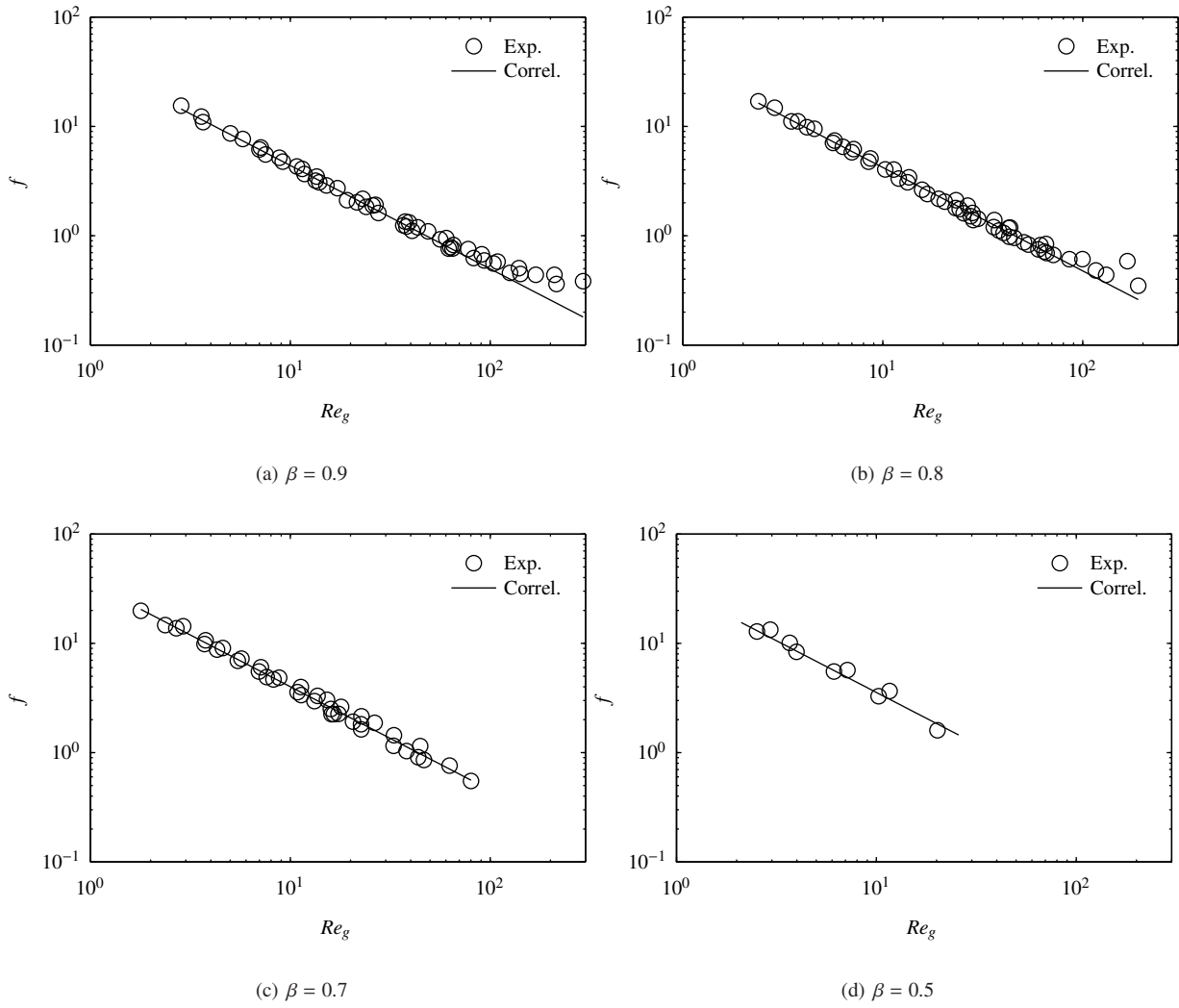


Figure 3: Experimental pressure drop measurements and correlation during the co-current movement of the scraper. Correlation according to Eq. 7 and Table 1(a).

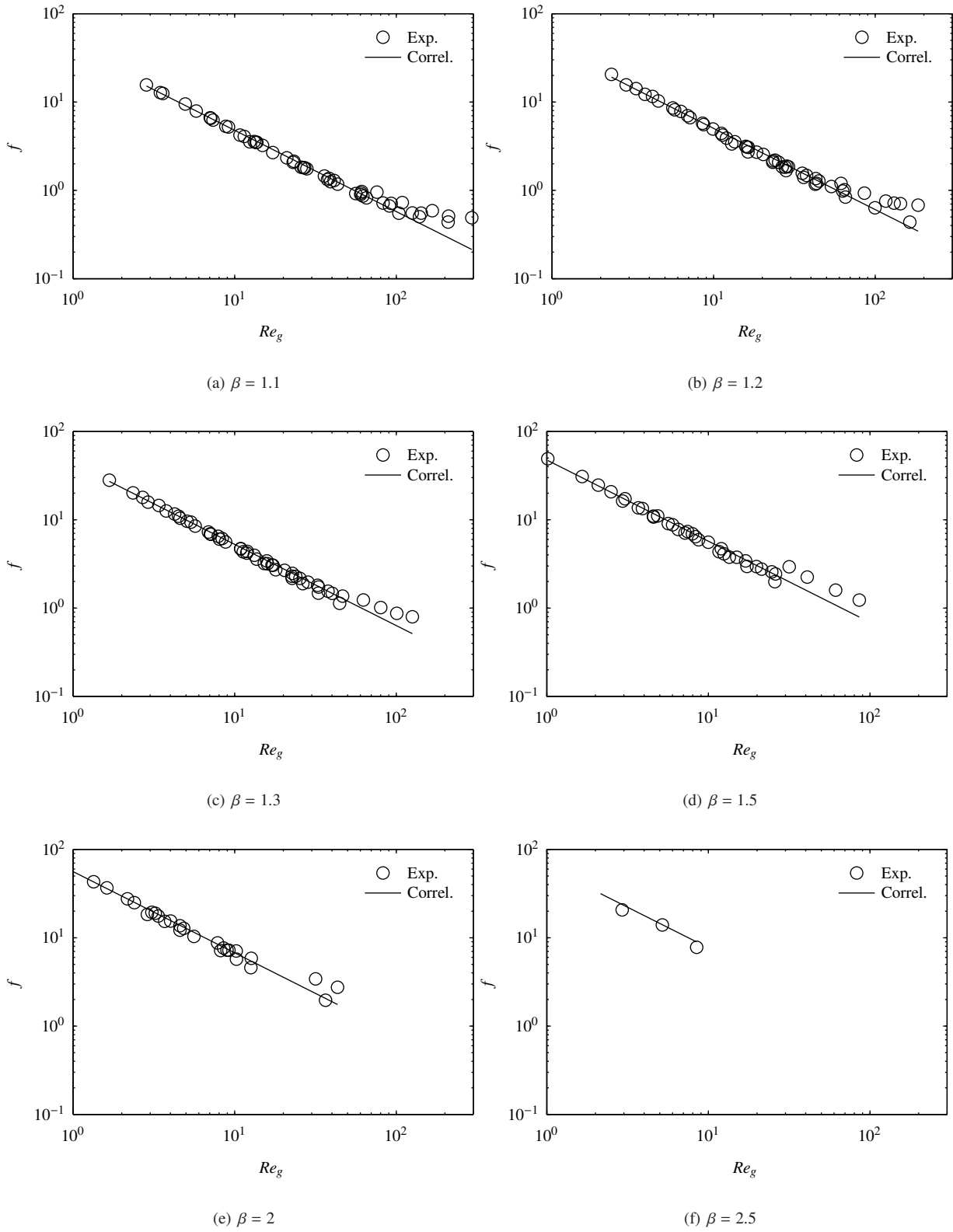


Figure 4: Experimental pressure drop measurements and correlation during the counter-current movement of the scraper. Experimental correlation according to Eq. 7 and Table 1(a)..

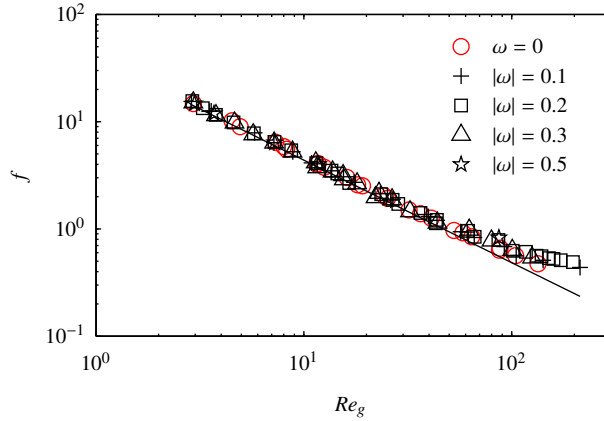


Figure 5: Full cycle average pressure drop and experimental correlations for the laminar flow region (Table 1(b)).

212 velocity will be used for the analysis:

$$\omega = v_s/u_b \quad (8)$$

213 Experiments have been carried out at Reynolds numbers within the range  $Re_g \in [1; 200]$ , at different scraping  
 214 velocities  $|\omega| = 0.1; 0.2; 0.3; 0.5$ , being the rheological properties of the fluid within the ranges  $n \in [0.45; 1]$  and  
 215  $m \in [4.53; 0.1] \text{ Pa s}^n$ .

216 The results in Fig. 5 show that, within the analysed range, the impact of the scraping velocity on the average  
 217 pressure drop in the laminar region is not significant. Therefore, the experiments have been correlated (Table 1(b)) to

$$f = a_2 Re_g^{b_2} \quad (9)$$

218 For experiments with higher non-dimensional scraping velocity  $\omega$ , the transition is observed to occur for lower  
 219 Reynolds numbers. Besides, for high Reynolds numbers, experiments with higher  $\omega$  show higher pressure drop.

220 The results of the experiments with the static scraper within the same range of Reynolds numbers has been plotted  
 221 in Fig. 5 as well. The data shows that, in the laminar flow region, there is no significant difference between the pressure  
 222 drop in static and dynamic conditions of the scraper within the analysed ranges.

## 223 5. Heat transfer results

224 Heat transfer to pseudoplastic non-Newtonian fluids has been analysed in static and dynamic conditions of the  
 225 scraper.

### 226 5.1. Heat Transfer in static conditions

227 Pseudoplastic fluids with rheological properties in the ranges  $n \in [0.45; 0.94]$  and  $m \in [4.6; 0.04] \text{ Pa.s}^n$  have been  
 228 used as test fluid for heat transfer experiments in static conditions of the scraper. A total of 120 experiments, grouped

Table 2: Static conditions heat transfer experiments.

(a) Experiment sets characteristics.

Exp	$T$ ( $^{\circ}\text{C}$ )	$n$	$m$ ( $\text{Pa}\cdot\text{s}^n$ )	$Pr_g$	$Pr_{g,ref}$
HT1	20	0.85 – 0.82	0.1091 – 0.2297	415 – 550	500
HT2	18	0.86 – 0.84	0.1244 – 0.1836	394 – 529	470
HT3	35	0.79 – 0.8	0.2216 – 0.1838	307 – 481	390
HT4	35	0.93 – 0.94	0.0488 – 0.0433	180 – 201	190
HT5	15	0.45 – 0.45	4.571 – 4.527	1240 – 4500	2960
HT6	25	0.46 – 0.47	3.873 – 3.470	967 – 4240	2400
HT7	35	0.52 – 0.52	2.113 – 2.093	637 – 2560	1430
HT8	15	0.60 – 0.60	1.439 – 1.371	712 – 2110	1320
HT9	25	0.62 – 0.64	1.026 – 0.886	556 – 1510	940
HT10	35	0.69 – 0.70	0.5510 – 0.4820	413 – 865	630
HT11	25	0.74 – 0.74	0.3810 – 0.3622	396 – 721	550

(b) Correlation constants (Eq. 10).

Flow Region	$a_3$	$b_3$	$c_3$	$U(Nu)$
I	0.4037	0.3735	0.3002	4.8%
II	0.4148	0.5921	0.2352	7.4%
IV	0.0259	1.1107	0.2354	19.8%

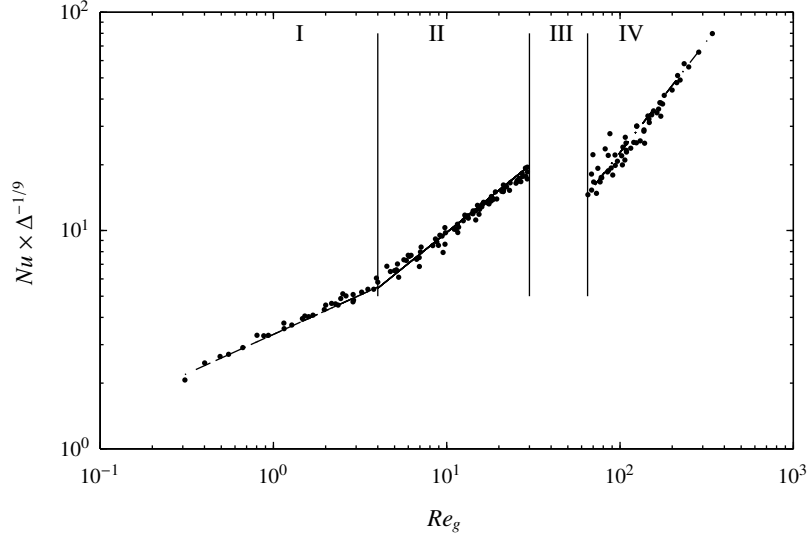


Figure 6: Flow regions. All the experiment results have been transported to  $Pr_g = 1000$  by using Eq. 10. Results at region III cannot be transported.

229 in 11 sets, have been carried out within the following ranges of Reynolds and Prandtl numbers:  $Re_g \in [0.4; 320]$  and  
 230  $Pr_g \in [180; 4500]$ . The properties of the experiments within a set are detailed in Table 2(a).

231 For the results, four regions of the fluid have been identified:

- 232 • *Region I.* Laminar attached flow.
- 233 • *Region II.* Laminar detached flow.
- 234 • *Region III.* Transition from laminar to turbulent flow.
- 235 • *Region IV.* Turbulent flow.

236 The obtained results have been correlated to the Eq. 10, where the  $\Delta$  parameter has been defined in Section 2.

$$Nu = a_3 Re_g^{b_3} Pr_g^{c_3} \Delta^{1/9} \quad (10)$$

237 On the one hand, the correlation constants are shown in Table 2(b) for all the regions of the fluid but the transition  
 238 one. On the other hand, the fluid regions are shown in Fig. 6, where, for a better understanding, the results for all the  
 239 experiments have been transported to  $Pr_g = 1000$ , by using Eq. 10.

240 By using a non-Newtonian highly viscous fluid, valuable data have been obtained for very low Reynolds. This  
 241 has permitted us to identify two different laminar regions (I and II). Region I is defined for  $Re_g < 4$ , while region II is  
 242 defined for  $4 < Re_g < 30$ . In region I, the boundary layer is attached to the boundary solids, while in region II there  
 243 is a boundary layer detachment downstream each semicircular piece, but the flow remains laminar (Crespí-Llorens  
 244 et al., 2016).

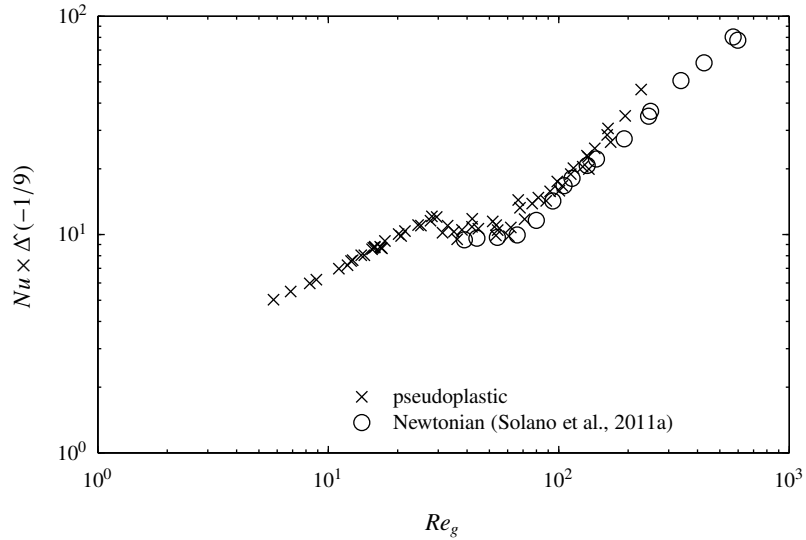


Figure 7: Validation of the heat transfer results in static conditions of the scraper by comparison with equivalent results with Newtonian flows at  $Pr_g = 300$ . The results correspond to experiment sets HT1, HT2, HT3 and HT11.

245 As it can be observed in Fig. 6, the Nusselt number dependence on the Reynolds number is lower in region I than  
 246 in region II. This is due to the differences in the flow pattern in regions I and II. The more important is the boundary  
 247 layer detachment after the semicircular pieces, the higher the heat transfer enhancement. It is noteworthy that no  
 248 differences have been found between regions I and II in pressure drop results.

249 The transition to the turbulent flow begins at  $Re_g \approx 30$  and the flow is fully turbulent (region IV) for  $Re_g >$   
 250  $65$ . In region III (transitional flow), the Nusselt number has a low dependence on the Reynolds number and higher  
 251 dependence on the Prandtl number, but no correlation can be obtained for this region, due to the high variability of the  
 252 results.

253 The validation of the results in Fig 7 has been carried out by comparing them to the ones obtained by Solano et al.  
 254 (2011a) for Newtonian fluids inside the same device for Prandtl numbers  $Pr = Pr_g = 300$ . The comparison is shown  
 255 in Fig. 7. Despite the difference in the viscosity of the fluids, the results overlap in region III and part of region IV,  
 256 showing a good matching.

## 257 5.2. Heat Transfer in dynamic conditions

258 In dynamic conditions of the scraper, a total of 197 experiments in 9 sets (Table 3(a)) have been carried out at  
 259 low scraping velocities  $|\omega| \in [0.1; 1]$  within the following ranges:  $Re_g \in [1.3; 216]$  and  $Pr_g \in [215; 2600]$ . For that,  
 260 pseudoplastic test fluids with rheological properties within the ranges  $n \in [0.45; 0.94]$  and  $m \in [4.6; 0.04]$  Pa.s<sup>n</sup> have  
 261 been used.

262 As in subsection 5.1, four flow regions have been identified with equivalent characteristics. The results in regions



Table 3: Dynamic conditions heat transfer experiments.

(a) Experiments sets characteristics.

Exp	$T$ ( $^{\circ}\text{C}$ )	$n$	$m$ ( $\text{Pa}\cdot\text{s}^n$ )	$Pr_g$
DHT-1	16.17 – 17.23	0.48 – 0.53	2.862 – 1.928	215 – 2120
DHT-2	16.9 – 17.61	0.59 – 0.63	1.292 – 0.8988	632 – 1450
DHT-3	16.7 – 16.3	0.81 – 0.82	0.2235 – 0.1907	410 – 600
DHT-4	17.2 – 18	0.93 – 0.94	0.0624 – 0.0551	250 – 290
DHT-5	25.8 – 25.5	0.75 – 0.74	0.3478 – 0.3588	456 – 746
DHT-6	16.9 – 16	0.69 – 0.71	0.6303 – 0.5910	630 – 1070
DHT-7	17.6 – 17.0	0.52 – 0.52	2.640 – 2.557	790 – 2625
DHT-8	18.0 – 17.7	0.62 – 0.64	1.164 – 0.9691	700 – 1590
DHT-9	15.8 – 15.8	0.87 – 0.89	0.1267 – 0.1118	330 – 425

(b) Correlation constants (Eq. 11).

Region	$Re_g$	$a_4$	$b_4$	$c_4$	$d_4$	$e_4$	$N$	$U(Nu)$
I	1 – 4	0.0212	0.6677	0.6102	1.2401	1.5544	26	15.1%
II	4 – 30	0.2584	0.5989	0.3702	0.6511	0.9300	147	6.6%
IV	> 50	0.0566	0.8977	0.3820	$2.2 \times 10^{-10}$	0.0179	24	21.7%

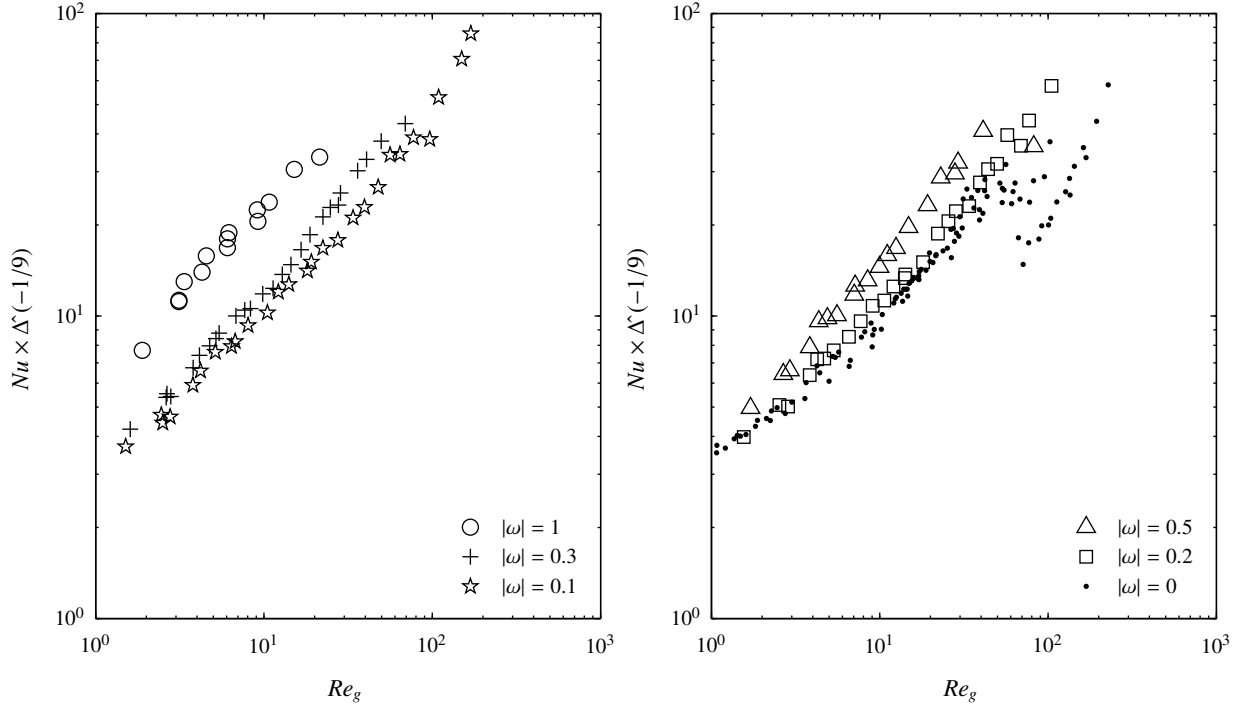


Figure 8: Scraping velocity effect on the Nusselt Number. Experimental data has been transported to  $Pr_g = 1000$ .

263 I, II and IV have been correlated to Eq. 11 and the constants results are shown in Table 3(b). The average value of  $\Delta$   
 264 in both scraping cycles for an annulus geometry is practically equal to the one of the static case, so the latter has been  
 265 used.

$$Nu = a_4 Re_g^{b_4} Pr_g^{c_4} (d_4 + |\omega|)^{e_4} \Delta^{1/9} \quad (11)$$

266 The values of the correlation constants in Table 3(b) show that the influence of the Reynolds number and Prandtl  
 267 numbers are similar to the ones in the static case, while the movement of the scraper produces heat transfer enhance-  
 268 ment in all fluid regions. In order to observe the latter, heat transfer results for different scraping velocities (including  
 269 the static case for  $\omega = 0$ ) are shown in Fig. 8. The figure shows as well that the transitional flow region is smaller, the  
 270 greater the scraping velocity.

271 The validation step is carried out again by comparing results to the existing ones for Newtonian fluids (Solano  
 272 et al., 2011b) for similar Prandtl numbers. Such comparison is shown in Fig. 9. Once again, the influence of the  
 273 non-Newtonian fluid behaviour is characterized by the definitions of the generalized viscosity  $\mu_g$  and the parameter  $\Delta$ .

274 Besides, Fig. 7 and Fig. 9 show the different working ranges of Reynolds numbers for Newtonian and non-  
 275 Newtonian fluids. Although the viscosity depends on the working fluid and the working conditions, the compared

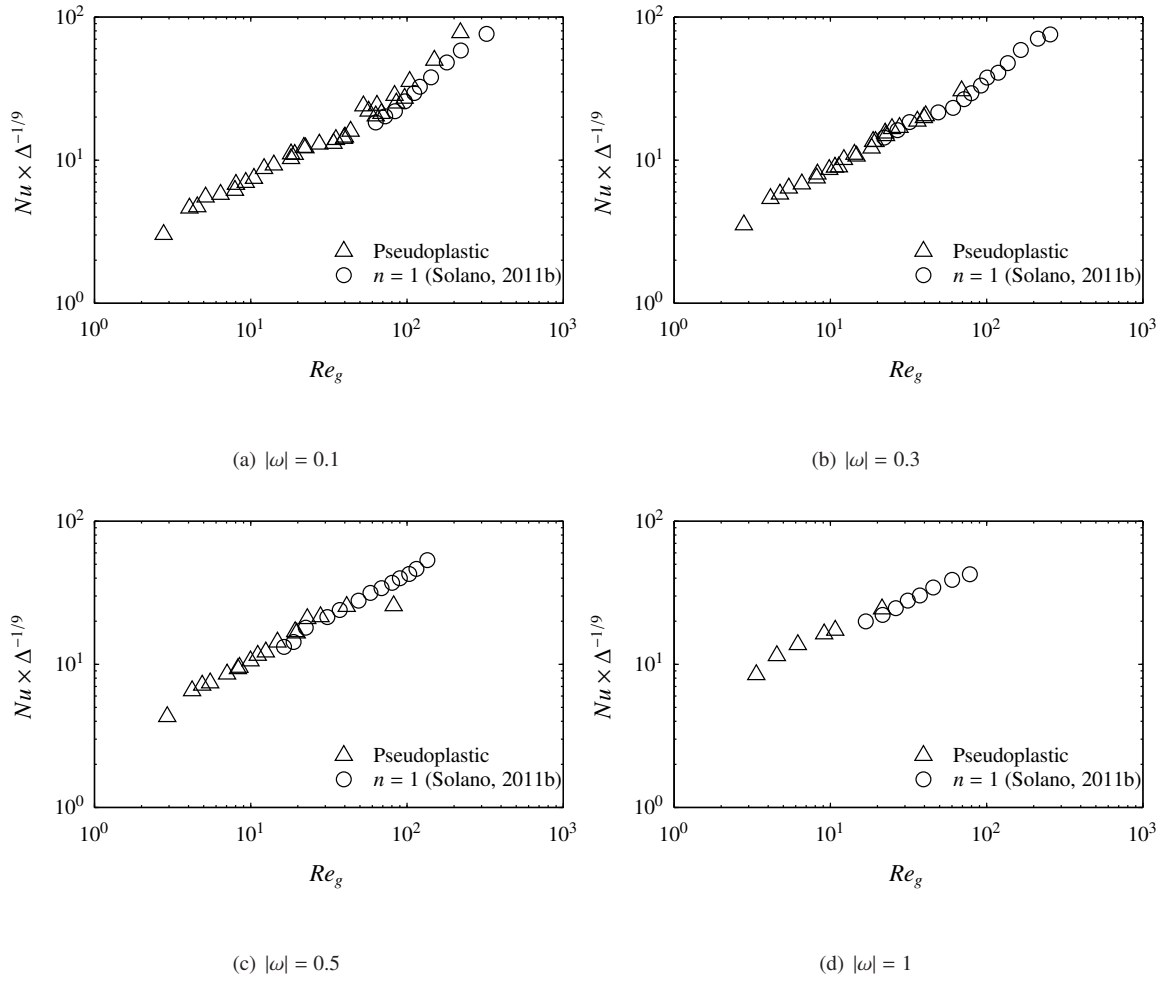


Figure 9: Comparison of Nusselt number results working with pseudoplastic (transported to  $Pr_g = 450$ ) and Newtonian fluids ( $Pr = 450$ ).

276 cases are very representative of the fluids in the process industry, as non-Newtonian fluids are usually significantly  
 277 more viscous than Newtonian fluids.

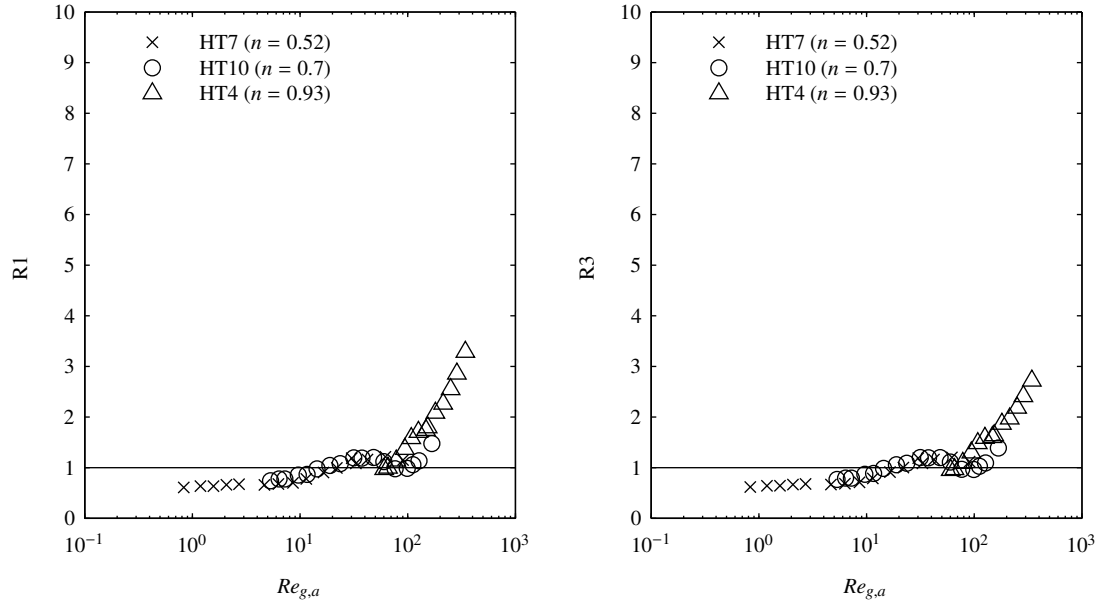


Figure 10: Performance evaluation of the scraper in static conditions. Static scraper vs. pure forced convection in a smooth pipe .

## 278 6. Performance evaluation of the device

279 The overall performance of the device has been evaluated in static and dynamic conditions of the scraper. To that  
 280 end, two classic criteria defined by Bergles et al. (1974) and Webb (1981) have been used:

- 281 • R1 criterion: Shows the heat transfer enhancement for the same flow rate and exchange area ( $Q_a/Q_{sp} = 1$ ,  
 282  $\dot{A}_a/\dot{A}_{sp} = 1$ ).
- 283 • R3 criterion: Shows the heat transfer enhancement for the same power consumption and exchange area ( $\dot{W}_a/\dot{W}_{sp} =$   
 284  $1$ ,  $\dot{A}_a/\dot{A}_{sp} = 1$ ). In this criterion, the consumption of the circulating pump and the rod propelling system (in  
 285 dynamic conditions of the scraper) have been considered.

### 286 6.1. Performance evaluation in static conditions

287 The performance of the device under study has been compared to a *smooth pipe* of the same length and with a  
 288 diameter equal to the hydraulic diameter of the device under study ( $D_h$ ). However, it should be taken into account,  
 289 that in the applications for which the current device is intended, a simple pipe heat exchanger is not an option, due to  
 290 the strong fouling formation.

291 The comparison has been carried out by using both the R1 and the R3 criteria. Both R1 and R3 criteria are  
 292 formulated as a Nusselt number ratio.

293 The R1 criterion compares situations which comply with the following relation between Reynolds numbers

$$\frac{Re_{g,sp}}{Re_{g,a}} = \frac{\phi_a(n)}{\phi_{sp}(n)} \left( \frac{D+d}{D_h} \right)^{2-n} \quad (12)$$

294 and the R3 criterion compares situations which comply with

$$\frac{Re_{g,sp}}{Re_{g,a}} = \frac{\phi_a(n)}{\phi_{sp}(n)} \left[ \frac{f_a}{f_{sp}} \left( 1 + \frac{d}{D} \right) \right]^{(2-n)/3} \quad (13)$$

295 The R1 criterion in Fig 10 shows heat transfer enhancements for the scraper for  $Re_{g,a} > 20$  which approximately  
 296 corresponds to the beginning of region III, being very significant for turbulent flow regimes (region IV,  $Re_{g,a} > 65$ ),  
 297 where heat transfer has increased up to more than 3 times. The main reason for this enhancement is that the presence  
 298 of the semicircular plugs causes the transition to turbulent flow to take place for much lower Reynolds numbers than  
 299 in the smooth pipe. However, for low Reynolds numbers ( $Re_{g,a} < 20$ ) the scraper lessens heat transfer. This is due to  
 300 the presence of the plastic semicircular plugs which have poor heat conductivity.

301 The R3 comparison shows similar results to the R1 comparison. However, as the scraper increases pumping  
 302 requirements, the R3 shows lower heat transfer enhancement than the R1 criterion (up to 2.8 times versus up to 3.4  
 303 times).

## 304 6.2. Performance evaluation of the scraping movement

305 In this section, the performance of the device under dynamic conditions of the scraper has been evaluated. To that  
 306 end, its performance in dynamic conditions has been compared to its performance in static conditions. This way, the  
 307 choices of continuously actuating the scraper at different velocities or only sporadically to remove fouling, have been  
 308 evaluated.

309 Firstly, the R1 criterion is plotted in Fig. 11. The results show that actuating the insert device enhances heat  
 310 transfer in any case. Besides, the faster the insert device moves alternately, the greater heat transfer enhancement is  
 311 obtained within the studied range of scraping velocities ( $|\omega| \in [0.1; 1]$ ). Heat transfer enhancements in the laminar  
 312 flow regions (referring to the case of the static scraper) can be up to 1.2 times for a scraping velocity of  $|\omega| = 0.2$ , up  
 313 to 1.7 times for  $|\omega| = 0.5$  and up to 2.5 times for  $|\omega| = 1$ . Furthermore, for the turbulent flow region (referred to the  
 314 case of the static device), heat transfer enhancements are far greater, reaching values of 1.8 times for  $|\omega| = 0.2$  and 2.4  
 315 times for  $|\omega| = 0.5$ . Nonetheless, only a few values have been obtained for this region, due to the high viscosity of the  
 316 test fluid.

317 Secondly, the R3 criterion has been plotted in Fig. 12 for sets of experiments with different fluid rheology. This  
 318 criterion takes into account the energy consumption of both the pumping system and the propelling system for the  
 319 rod, by comparing situations with the same energy consumption. The results show that, as a general rule for the  
 320 experiments which have been carried out, for  $Re_{g,dy} < 50$ , and without taking fouling into account, it is energetically  
 321 not interesting to continuously actuate the device. However, for the experiments with higher Reynolds numbers, it  
 322 will be energetically interesting to actuate the scraping device at low scraping velocities in order to minimize power  
 323 consumption. For the fluid with the strongest pseudoplastic behaviour (DHT-1,  $n \approx 0.5$ ),  $R3 > 1$  for about  $Re_{g,dy} > 50$ ,  
 324 while for the almost Newtonian fluid (DHT-4,  $n \approx 0.93$ ),  $R3 > 1$  for about  $Re_{g,dy} > 120$ . From this, it can be concluded  
 325 that the limiting Reynolds number for the R3 criterion decreases with the pseudoplasticity of the fluid.

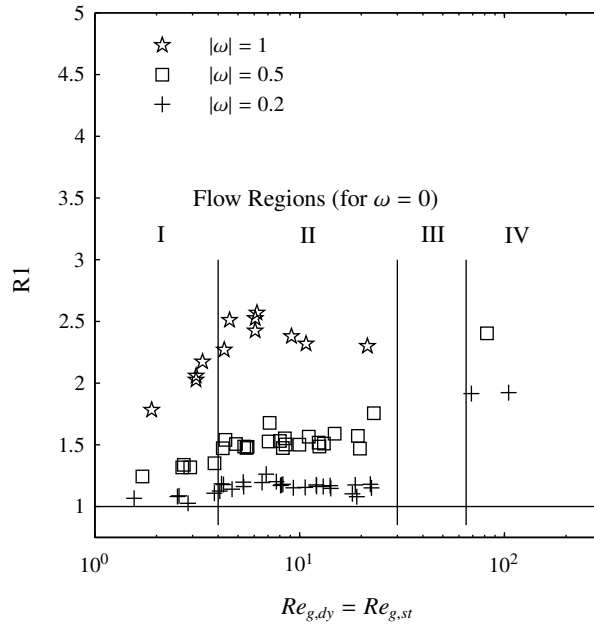


Figure 11: Performance evaluation of the scraper movement by using the R1 criterion. Dynamic vs. static conditions.

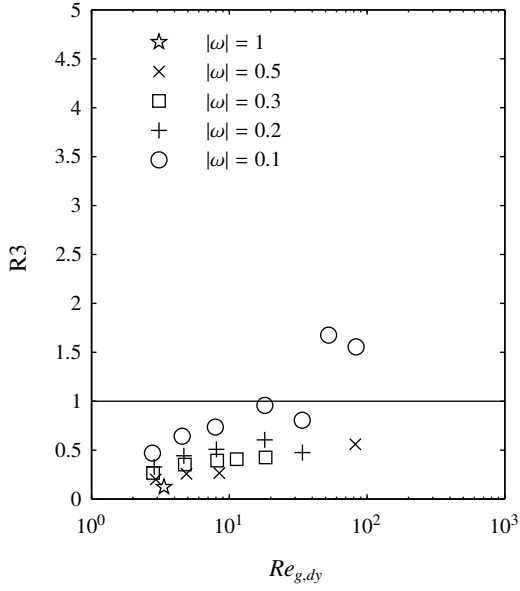
## 326 7. Conclusions

327 After analysing the obtained results as a whole, it can be concluded that the scraper is suitable to work with non-  
 328 Newtonian fluids. However, the recommended working ranges depend on many factors which shall be studied for  
 329 each case individually. Working in static conditions is energetically the most efficient solution, however, to avoid or  
 330 prevent fouling, some scraping movement will be required sporadically or continuously.

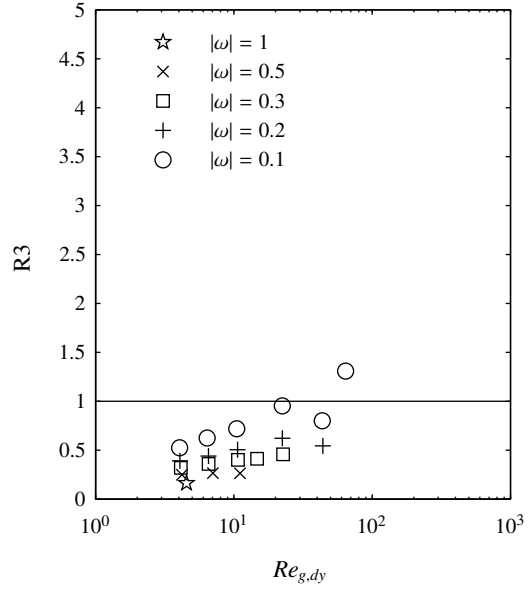
331 The movement of the insert device has been proved to produce heat transfer increase in any situation which has  
 332 been studied, although significantly increasing power consumption. The foregoing can be useful to control very  
 333 precisely heat transfer in an industrial process. Furthermore, some products, especially in the food industry, need to  
 334 be at a quite uniform temperature: if the product reaches too high temperatures near the wall, its quality will decrease  
 335 significantly and can even boost fouling formation.

336 The main conclusions of this research are summarized next:

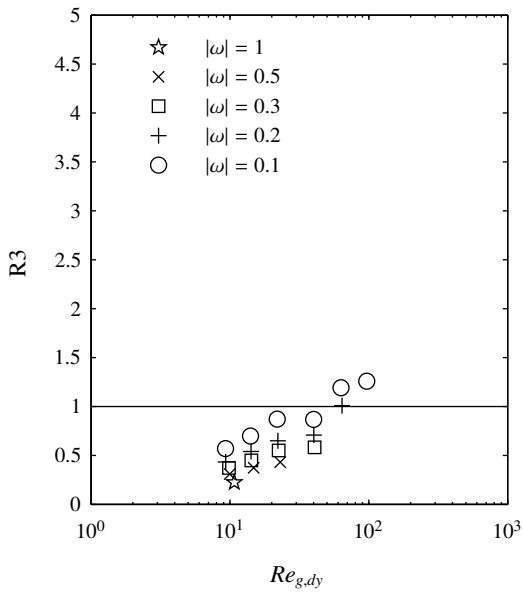
- 337 • Pressure drop, heat transfer and power consumption measurements, using non-Newtonian pseudoplastic fluids,  
 338 have been carried out in static and dynamic conditions of the scraper.
- 339 • Four flow regions have been identified: attached laminar, detached laminar, transitional and turbulent flow  
 340 regions.



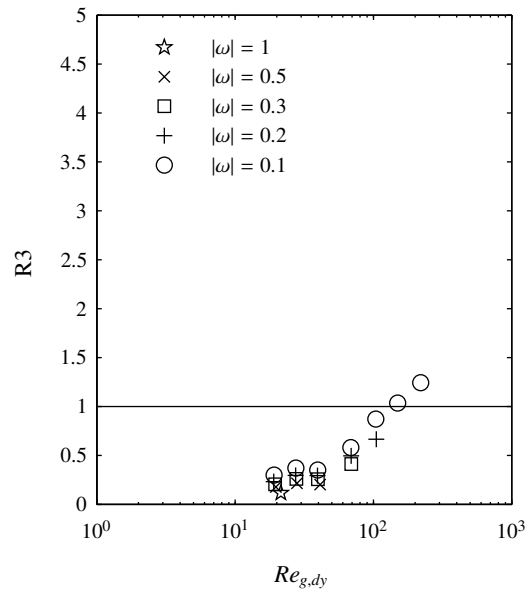
(a) DHT1,  $n \approx 0.5$  y  $m \approx 2.4 \text{ Pa.s}^n$



(b) DHT2,  $n \approx 0.61$  y  $m \approx 1.1 \text{ Pa.s}^n$



(c) DHT3,  $n \approx 0.81$  y  $m \approx 0.2 \text{ Pa.s}^n$



(d) DHT4,  $n \approx 0.93$  y  $m \approx 0.06 \text{ Pa.s}^n$

Figure 12: Dynamic vs. static scraper. R3 criterion. At the x-axis,  $Re_{g,dy}$  corresponding to dynamic experiments is plotted.

- 341 • A generalization method for the fluid viscosity, that includes the effects of the non-Newtonian fluid behaviour,  
342 has been used.
- 343 • The friction factor and the Nusselt number have been successfully correlated by employing the generalized  
344 viscosity on pressure drop and heat transfer results, both in static and dynamic conditions and for three of the  
345 four identified flow regions (it was not possible to get correlations in the transitional region).
- 346 – The friction factor depends on the generalized Reynolds number and on the blockage of the flow.
  - 347 – The Nusselt number in static and dynamic conditions has been found to depend on the generalized  
348 Reynolds number, the generalized Prandtl number, the non-dimensional scraping velocity and the non-  
349 Newtonian behaviour of the flow.
- 350 • Under no-fouling conditions, the device in static conditions is found to perform better than a smooth pipe  
351 heat exchanger for Reynolds numbers over 10, reaching significant heat transfer enhancements if the turbulent  
352 region is reached. Furthermore, actuating the scraper increases heat transfer in any case, but also increases  
353 energy consumption.
- 354 • The device is suitable for an industrial process using non-Newtonian fluids, since it prevents fouling, increases  
355 heat transfer, provides flexibility and enhances the final product quality. Furthermore, the obtained correlations  
356 are a valuable tool in the design of heat exchangers.

## 357 **8. Acknowledgements**

358 This work was supported by the Ministry of Education of the Spanish Government [AP2007-03429], which cov-  
359 ered the expenses of a 4-year research at *Universidad Politécnica de Cartagena*, as well as a stage at the University of  
360 Sheerbroke in Canada, where part of this research was carried out. It was further covered by the Ministry of Science  
361 and Innovation (DPI2007-66551-C02-01).



362 Abdelrahim, K.A., Ramaswamy, H.S., 1995. High temperature/pressure rheology of carboxymethyl cellulose (CMC). *Food Research International*  
363 28, 285–290.

364 Abu-Jdayil, B., 2003. Modelling the time-dependent rheological behavior of semisolid foodstuffs. *Journal of Food Engineering* 57, 97–102.

365 Bergles, A., Blumenkrantz, A.R., Taborek, J., 1974. Performance evaluation criteria for enhanced heat transfer surface. *Journal of Heat Transfer* 2  
366 , 239–243.

367 Beuf, M., Rizzo, G., Leuliet, J., H.Müller-Steinhagen, Karabelas, A., Yiantsios, S., Benezech, T., 2003. Fouling and cleaning of modified stainless  
368 steel plate heat exchangers processing milk products, in: *Heat Exchanger Fouling and Cleaning: Fundamentals and Applications*.

369 Blél, W., Legentilhomme, P., Bénézéché, T., Fayolle, F., 2013. Cleanability study of a scraped surface heat exchanger. *Food and Bioproducts*  
370 *Processing* 91, 95 – 102.

371 Cancela, M., Alvarez, E., Maceiras, R., 2005. Effects of temperature and concentration on carboxymethylcellulose with sucrose rheology. *Journal*  
372 *of Food Engineering* 71, 419–424.

373 Chhabra, R., Richardson, J., 2008. *Non-Newtonian flow and applied rheology. Engineering applications*. Butterworth-Heinemann, 225 Wildwood  
374 Av., Woburn.

375 Crespí-Llorens, D., Vicente, P., Viedma, A., 2015. Generalized Reynolds number and viscosity definitions for non-Newtonian fluid flow in ducts  
376 of non-uniform cross-section. *Experimental Thermal and Fluid Science* 64, 125–133.

377 Crespí-Llorens, D., Vicente, P., Viedma, A., 2016. Flow pattern of non-Newtonian fluids in reciprocating scraped surface heat exchangers. *Exper-*  
378 *imental Thermal and Fluid Science* 76, 306 – 323.

379 De Goede, R., De Jong, E., 1993. Heat transfer properties of a scraped-surface heat exchanger in the turbulent flow regime. *Chemical Engineering*  
380 *Science* 48, 1393–1404.

381 Delplace, F., Leuliet, J., 1995. Generalized Reynolds number for the flow of power law fluids in cylindrical ducts of arbitrary cross-section. *The*  
382 *Chemical Engineering Journal and the Biochemical Engineering Journal* 56, 33 – 37.

383 Fyrippi, I., Owen, I., Escudier, M., 2004. Flowmetering of non-Newtonian liquids. *Flow Measurement and Instrumentation* 15, 131–138.

384 Ghannam, M.T., Esmail, M.N., 1996. Rheological properties of carboxymethyl cellulose. *Journal of Applied Polymer Science* 64, 289–301.

385 Griggull, U., 1956. Wärmeübergang an nicht-newtonsche flüssigkeiten bei laminarer rohströmung. *Chemie Ingenieur Technik* 28, 553–556.

386 ISO, 1995. *Guide to the Expression for Uncertainty Measurement*, first ed. International Organization for Standardization, Switzerland.

387 Joshi, S., Bergles, A., 1980. Experimental study of laminar heat transfer to in-tube flow of non-Newtonian fluids. *Journal of Heat Transfer* 102,  
388 397–401.

389 Joshi, S.D., 1978. Heat transfer in in-tube flow of non-Newtonian fluids. Ph.D. thesis. Iowa State University. Ames, Iowa.

390 Kozicki, W., Chou, C.H., Tiu, C., 1966. Non-Newtonian flow in ducts of arbitrary cross-sectional shape. *Chemical Engineering Science* 21, 665 –  
391 679.

392 Mabit, J., Fayolle, F., Legrand, J., 2003. Shear rates investigation in a scraped surface heat exchanger. *Chemical Engineering Science* 58, 4667 –  
393 4679.

394 Martínez, D., García, A., Solano, J., Viedma, A., 2014. Heat transfer enhancement of laminar and transitional Newtonian and non-Newtonian flows  
395 in tubes with wire coil inserts. *International Journal of Heat and Mass Transfer* 76, 540–548.

396 Metzner, A., 1965. Heat transfer in non-Newtonian fluids, in: Hartnett, J., T. F. Irvine, J. (Eds.), *Advances in Heat Transfer*. Academic Press, New  
397 York. volume 2, pp. 357–397.

398 Metzner, A.B., Reed, J.C., 1955. Flow of non-Newtonian fluids - correlation of the laminar, transition, and turbulent-flow regions. *Aiche Journal*  
399 1(4), 434–440.

400 Solano, J.P., García, A., Vicente, P.G., Viedma, A., 2011a. Flow field and heat transfer investigation in tubes of heat exchangers with motionless  
401 scrapers. *Applied Thermal Engineering* 31, 2013 – 2024.

402 Solano, J.P., García, A., Vicente, P.G., Viedma, A., 2011b. Flow pattern assessment in tubes of reciprocating scraped surface heat exchangers.  
403 *International Journal of Thermal Sciences* 50, 803 – 815.

404 Sun, K., Pyle, D., Fitt, A., Please, C., Baines, M., Hall-Taylor, N., 2004. Numerical study of 2D heat transfer in a scraped surface heat exchanger.

405 Computers and Fluids 33, 869–880.

406 Wang, W., Walton, J., McCarthy, K., 1999. Flow profiles of Power Law fluids in scraped surface heat exchanger geometry using MRI. *Journal of*  
407 *Food Process Engineering* 22, 11–27.

408 Webb, R., 1981. Performance evaluation criteria for use of enhanced heat transfer surface in heat exchanger design. *International Journal of Heat*  
409 *and Mass Transfer* 24, 715–726.

410 Yang, X.H., Zhu, W.L., 2007. Viscosity properties of sodium carboxymethylcellulose solutions. *Cellulose* .

411 Yataghene, M., Fayolle, F., Legrand, J., 2009. Experimental and numerical analysis of heat transfer including viscous dissipation in a scraped  
412 surface heat exchanger. *Chemical Engineering and Processing: Process Intensification* 48, 1447 – 1458.

413 Yataghene, M., Francine, F., Jack, L., 2011. Flow patterns analysis using experimental PIV technique inside scraped surface heat exchanger in  
414 continuous flow condition. *Applied Thermal Engineering* 31, 2855 – 2868.

415 Yataghene, M., Pruvost, J., Fayolle, F., Legrand, J., 2008. CFD analysis of the flow pattern and local shear rate in a scraped surface heat exchanger.  
416 *Chemical Engineering and Processing: Process Intensification* 47, 1550 – 1561.

417 **List of Figures**

418 1 Device under study. . . . . 5

419 2 Experimental set-up. (1) Test fluid tank, (2) primary loop gear pump, (3) frequency converter, (4)

420 immersion resistance, (5) Coriolis flowmeter, (6) RTD temperature sensor, (7) non-stationary differ-

421 ential piezoresistive pressure transmitters, (8) stainless steel tube with an insert scraper and with inlet

422 and outlet immersion RTDs, (9) pressure taps, (10) electric transformer, (11) electrodes, (12) smooth

423 stainless steel pipe used as viscometer, (13) stationary pressure transmitters, (14) hydraulic piston,

424 (15) non-stationary bidirectional differential piezoresistive pressure transmitter, (16) heat exchanger,

425 (17) cooling loop gear pump, (18) three-way valve with a PID controller, (19) coolant liquid tank, (20)

426 centrifugal pump. . . . . 6

427 3 Experimental pressure drop measurements and correlation during the co-current movement of the

428 scraper. Correlation according to Eq. 7 and Table 1(a). . . . . 11

429 4 Experimental pressure drop measurements and correlation during the counter-current movement of

430 the scraper. Experimental correlation according to Eq. 7 and Table 1(a).. . . . . 12

431 5 Full cycle average pressure drop and experimental correlations for the laminar flow region (Table 1(b)). 13

432 6 Flow regions. All the experiment results have been transported to  $Pr_g = 1000$  by using Eq. 10. Results

433 at region III cannot be transported. . . . . 15

434 7 Validation of the heat transfer results in static conditions of the scraper by comparison with equivalent

435 results with Newtonian flows at  $Pr_g = 300$ . The results correspond to experiment sets HT1, HT2,

436 HT3 and HT11. . . . . 16

437 8 Scraping velocity effect on the Nusselt Number. Experimental data has been transported to  $Pr_g =$

438  $1000$ . . . . . 18

439 9 Comparison of Nusselt number results working with pseudoplastic (transported to  $Pr_g = 450$ ) and

440 Newtonian fluids ( $Pr = 450$ ). . . . . 19

441 10 Performance evaluation of the scraper in static conditions. Static scraper vs. pure forced convection

442 in a smooth pipe . . . . . 20

443 11 Performance evaluation of the scraper movement by using the R1 criterion. Dynamic vs. static con-

444 ditions. . . . . 22

445 12 Dynamic vs. static scraper. R3 criterion. At the  $x$ -axis,  $Re_{g,dy}$  corresponding to dynamic experiments

446 is plotted. . . . . 23